Synthesis, Structure, and Ethylene/α-Olefin Polymerization Behavior of (Cyclopentadienyl)(nitroxide)titanium Complexes

Mahesh K. Mahanthappa, Adam P. Cole, and Robert M. Waymouth*

Department of Chemistry, Stanford University, Stanford, California 94305-5080

Received August 6, 2003

Mono-Cp titanium coordination compounds bearing monoanionic ligands derived from stable nitroxyl radicals have been synthesized by two methods: (i) trapping of CpTi(III) species with the stable nitroxyl radical TEMPO (2,2,6,6-tetramethylpiperidine-*N*-oxyl) to provide $Cp'TiCl_2$(TEMPO) (Cp′ = Cp (**1**) and Cp* (**2**)) and (ii) salt metathesis of Ti(IV) halides with a nitroxide anion generated by the in situ methylation of *tert*-butyl-α-phenylnitrone. Alkylation of these complexes with MeLi or MeMgBr furnishes Cp^*TiMe_2(TEMPO) (**3**) and $Cp'TiMe_2(ON(^tBu)(CHMePh))$ (Cp′ = Cp(**4**) and Cp* (**5**)). The molecular structure of **2** has been determined by X-ray crystallography to reveal a monoanionic η^1-TEMPO ligated to titanium. Complexes **3** and **4** activated with ^{ipr}AFPB (2,6,-diisopropyl-*N*,*N*-dimethylanilinium tetrakis(pentafluorophenyl)borate) efficiently copolymerize ethylene and 1-hexene to provide copolymers having higher 1-hexene contents and higher productivities than the related $Cp^*Ti(CH_2Ph)_3$ under identical conditions. Comparison of structural and electronic features as well as the ethylene/1-hexene copolymerization behavior of **3** and **4** with the constrained geometry catalyst $[MeSi_2(\eta^5\text{-}Me_4Cp)(\eta^1\text{-N-}t\text{Bu})]TiMe_2$ (**6**) provides insights into factors governing high comonomer incorporation by mono-Cp titanium complexes.

Introduction

The development of homogeneous coordination polymerization catalysts has created new opportunities for the production of ethylene α-olefin copolymers.[1−4] The ligand environments of well-defined coordination compounds can be systematically varied to control the degree of comonomer incorporation and, in some cases, the comonomer distribution.[2,5−13] Correlations between catalyst structure and the microstructure of the resulting ethylene/α-olefin copolymers provide the ability to tailor important bulk polymer properties such as the melting points (T_m), the glass transition temperatures (T_g), crystallinities, densities, tensile strengths, and elastic moduli, thus impacting ultimate processability and applications of these industrially important materials.[3,4,14−22]

Recent studies of hybrid metallocene systems (sometimes referred to as “half-metallocenes”) having one cyclopentadienyl moiety and one monoanionic ligand have led to new classes of copolymerization catalysts.[23−35] In particular, the “constrained geometry” catalysts (CGCs) have proven to be a very successful

---

* To whom correspondence should be addressed. E-mail: waymouth@stanford.edu.

(1) Brintzinger, H. H.; Fischer, D.; Mulhaupt, R.; Rieger, B.; Waymouth, R. M. *Angew. Chem., Int. Ed. Engl.* **1995**, *34*, 1143−1170.

(2) Galimberti, M.; Piemontesi, F.; Fusco, O. In *Metallocene-Based Polyolefins*; Scheirs, J., Kaminsky, W., Eds.; Wiley: Chichester, 2000; Vol. 1; pp 309−343.

(3) Scheirs, J.; Kaminsky, W. *Metallocene-based Polyolefins: Preparation, Properties, and Technology*; John Wiley & Sons Ltd.: Chichester, 2000; Vol. 1.

(4) Scheirs, J.; Kaminsky, W. *Metallocene-based Polyolefins: Preparation, properties, and technology*; John Wiley & Sons Ltd.: Chichester, 2000; Vol. 2.

(5) Galimberti, M.; Piemontesi, F.; Fusco, O.; Camurati, I.; Destro, M. *Macromolecules* **1998**, *31*, 3409−3416.

(6) Galimberti, M.; Piemontesi, F.; Mascellani, N.; Camurati, I.; Fusco, O.; Destro, M. *Macromolecules* **1999**, *32*, 7968−7976.

(7) Arndt, M.; Kaminsky, W.; Schauwienold, A.-M.; Weingarten, U. *Macromol. Chem. Phys.* **1998**, *199*,

(8) Uozumi, T.; Miyazawa, K.; Sano, T.; Soga, K. *Macromol. Rapid Commun.* **1997**, *18*, 883−889.

(9) Uozumi, T.; Ahn, C. H.; Tomisaka, M.; Jin, J.; Tian, G.; Sano, T.; Soga, K. *Macromol. Chem. Phys.* **2000**, *201*, 1748−1752.

(10) Jin, J. H.; Uozumi, T.; Sano, T.; Teranishi, T.; Soga, K.; Shiono, T. *Macromol. Rapid Commun.* **1998**, *19*, 337−339.

(11) Leclerc, M. K.; Waymouth, R. M. *Angew. Chem. Int. Ed.* **1998**, *37*, 922−925.

(12) Fan, W.-H.; Leclerc, M. K.; Waymouth, R. M. *J. Am. Chem. Soc.* **2001**, *123*, 9555.

(13) Choo, T. N.; Waymouth, R. M. *J. Am. Chem. Soc.* **2002**, *124*, 4188−4189.

(14) Alamo, R. G., Mandelkern, L. *Thermochim. Acta* **1994**, *238*, 155−201.

(15) Alizadeh, A.; Richardson, L.; Xu, J.; McCartney, S.; Marand, H. *Macromolecules* **1999**, *32*, 6221−6235.

(16) Burfield, D. R. *Macromolecules* **1987**, *20*, 3020−3023.

(17) Simanke, A. G.; Alamo, R. G.; Galland, G. B.; Mauler, R. S. *Macromolecules* **2001**, *34*, 6959−6971.

(18) Simanke, A. G.; Galland, G. B.; Freitas, L. L.; da Jornada, J. A. H.; Quijada, R.; Mauler, R. S. *Macromol. Chem. Phys.* **2001**, *202*, 172−179.

(19) Schulze, U.; Arndt, M.; Freidanck, F.; Beulich, I.; Pompe, G.; Meyer, E.; Jehnichen, D.; Pionteck, J.; Kaminsky, W. *J. Macromol. Sci., Pure. Appl. Chem.* **1998**, *A35*, 1037−1044.

(20) Mouzakis, D. E.; Mader, D.; Mulhaupt, R.; KargerKocsis, J. *J. Mater. Sci.* **2000**, *35*, 1219−1230.

(21) Walter, P.; Trinkle, S.; Suhm, J.; Mader, D.; Friedrich, C.; Mulhaupt, R. *Macromol. Chem. Phys.* **2000**, *201*, 604−612.

(22) McCoy, M. *Chem. Eng. News* **2002**, *80*, 60−65.

(23) McKnight, A. L.; Waymouth, R. M. *Chem. Rev.* **1998**, *98*, 2587−2598.

(24) Sinnema, P. J.; Liekelema, K.; Staal, O. K. B.; Hessen, B.; Teuben, J. H. *J. Mol. Catal. A: Chem.* **1998**, *128*, 143−153.

(25) Nomura, K.; Oya, K.; Imanishi, Y. *J. Mol. Catal. A: Chem.* **2001**, *174*, 127−140.

(26) Nomura, K.; Fujii, K. *Organometallics* **2002**, *21*, 3042−3049.

(27) Von Haken Spence, R. E.; Stephan, D. W.; Brown, S. J.; Jeremic, D.; Wang, Q. PCT Int. Appl. 0005236, 2000.

10.1021/om034096s CCC: $27.50
Publication on Web 01/17/2004

Scheme 1

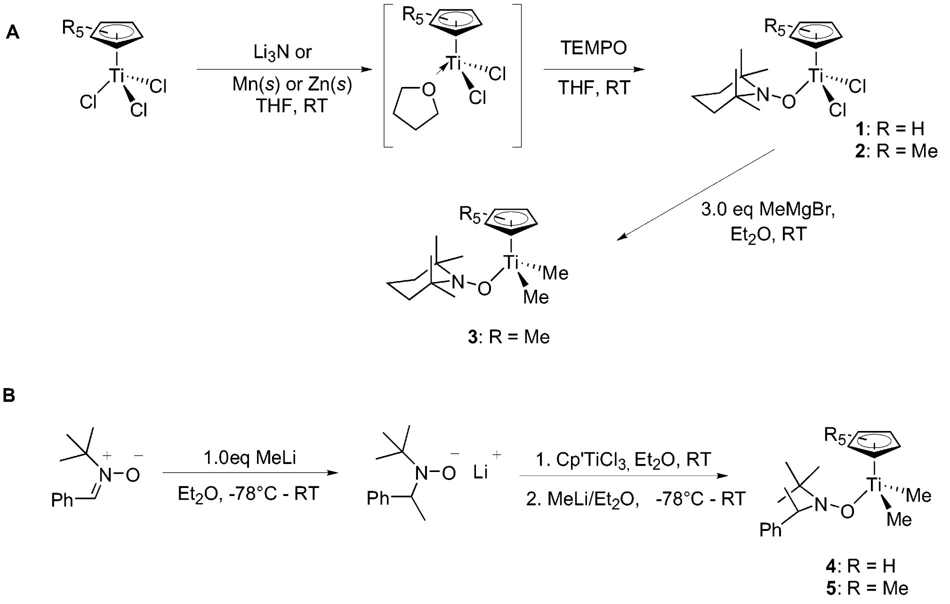

1: R = H
2: R = Me

3: R = Me

4: R = H
5: R = Me

class of catalysts which exhibit high activities and high comonomer incorporations.[23,36−38] The high comonomer incorporation ability of these complexes has been attributed to an open-coordination environment of these complexes, the "constrained geometry effect",[36,37] although recent work has called this notion into question.[33] Half-metallocene catalysts based on monocyclopentadienyl titanium complexes bearing monoanionic ligands such as tethered amides,[24,39] phosphinimides,[27,28,40,41] ketimides,[30,31] iminoimidazolidides,[29] aryloxides,[25,42−45] and hydroxylamines[35] are also effective catalysts for the efficient copolymerization of ethylene and 1-hexene.

We recently reported the synthesis of two titanium coordination compounds having ligands derived from the stable nitroxyl radical TEMPO (2,2,6,6,-tetramethylpiperidine-*N*-oxyl); X-ray analysis demonstrated that the nitroxyl ligand is reduced to generate a sterically encumbered monoanionic ligand whose binding mode depends sensitively on the ancillary ligation at titanium.[46] In this paper, we report the synthesis, structure, and ethylene/1-hexene copolymerization behavior of monocyclopentadienyl titanium complexes containing nitroxide ligands,[47] as well as the synthesis of a new, highly soluble organoboron cocatalyst for olefin polymerization.

Results and Discussion

Synthesis of CpTiR$_2$(nitroxide) Complexes. Monocyclopentadienyl titanium complexes containing nitroxide-derived ligands were synthesized by two distinct routes: (i) one-electron reduction of a CpTi(IV) fragment to a CpTi(III) species followed by trapping of the metalloradical with a nitroxyl radical (Scheme 1A) and (ii) treatment of a CpTi(IV) fragment with a nitroxide anion generated in situ from alkyllithium addition to nitrone (Scheme 1B).

In our previous work, we demonstrated that Ti(III) metalloradicals can be trapped with nitroxyl radicals to generate stable coordination complexes.[46] Stoichiometric reduction of CpTiCl$_3$ in tetrahydrofuran (THF) with Li$_3$N [48] generates CpTiCl$_2$(THF)$_x$ in situ, which can be trapped with TEMPO in THF to produce a dark red complex formulated as CpTiCl$_2$(TEMPO) (**1**) in 50% yield. The synthesis of Cp*TiCl$_2$(TEMPO) (**2**) was carried out by a similar procedure: Cp*TiCl$_3$ was reduced using excess Zn or Mn powder in THF to generate Cp*TiCl$_2$(THF) and trapped with TEMPO to yield dark

---

(28) Guerin, F.; Beddie, C. L.; Stephan, D. W.; Spence, R. E. v. H.; Wurz, R. *Organometallics* **2001**, *20*, 3466−3471.

(29) Kretschmer, W. P.; Dijkhuis, C.; Meetsma, A.; Hessen, B.; Teuben, J. H. *Chem. Commun.* **2002**, 608−609.

(30) Zhang, S.; Piers, W. E.; Gao, X. L.; Parvez, M. *J. Am. Chem. Soc.* **2000**, *122*, 5499−5509.

(31) McMeeking, J.; Gao, X.; Von Haken Spence, R. E.; Brown, S. J.; Jeremic, D. PCT Int. Appl. 9914250, 1999.

(32) Kunz, K., Erker, G., Döring, S., Bredeau, S., Kehr, G., Fröhlich, R. *Organometallics* **2002**, *21*, 1031−1041.

(33) Kunz, K.; Erker, G.; Kehr, G.; Frohlich, R.; Jacobsen, H.; Berke, H.; Blacque, O. *J. Am. Chem. Soc.* **2002**, *124*, 3316−3326.

(34) Kunz, M.; Erker, G.; Doring, S.; Bredeau, S.; Kehr, G.; Frohlich, R. *Organometallics* **2002**, *21*, 1031−1041.

(35) Nagy, S.; Etherton, B. P.; Krishnamurti, R.; Tyrell, J. A. U.S. Patent 6204216, 2001.

(36) Stevens, J. C. *Stud. Surf. Sci. Catal.* **1994**, *89*, 277−284.

(37) Stevens, J. C. In *Studies in Surface Science and Catalysis*; Hightower, J. W., Delglass, W. N., Iglesia, E., Bell, A. T., Eds.; Elsevier: Amsterdam, 1996; Vol. 101; pp 11−20.

(38) Galimberti, M.; Mascellani, N.; Piemontesi, F.; Camurati, I. *Macromol. Rapid Commun.* **1999**, *20*, 214−218.

(39) Sinnema, P. J.; Hessen, B.; Teuben, J. H. *Macromol. Rapid Commun.* **2000**, *21*, 562−566.

(40) Von Haken Spence, R. E.; Brown, S. J.; Wurz, R. P.; Jeremic, D.; Stephan, D. W. PCT Int. Appl. 0119512, 2001.

(41) Stephan, D. W.; Stewart, J. C.; Guerin, F.; Courtenay, S.; Kickham, J.; Hollink, E.; Beddie, C.; Hoskin, A.; Graham, T.; Wei, P.; Von Haken Spence, R. E.; Xu, W.; Koch, L.; Gao, X.; Harrison, D. G. *Organometallics* **2003**, *22*, 1937−1947.

(42) Nomura, K.; Komatsu, T.; Imanishi, Y. *J. Mol. Catal. A: Chem.* **2000**, *152*, 249−252.

(43) Nomura, K.; Naga, N.; Miki, M.; Yanagi, K. *Macromolecules* **1998**, *31*, 7588−7597.

(44) Thorn, M. G.; Vilardo, J. S.; Lee, J.; Hanna, B.; Fanwick, P. E.; Rothwell, I. P. *Organometallics* **2000**, *19*, 5636−5642.

(45) Thorn, M. G.; Etheridge, Z. C.; Fanwick, P. E.; Rothwell, I. P. *J. Organomet. Chem.* **1999**, *591*, 148−162.

(46) Mahanthappa, M. K.; Huang, K. W.; Cole, A. P.; Waymouth, R. M. *Chem. Commun.* **2002**, 502−503.

(47) The term "nitroxide" is used in this article to refer to the anion derived from a stable nitroxyl radical. These ligands are alternatively described as "hydroxylaminato" ligands in the literature.

(48) Kilner, M.; Parkin, G. *J. Organomet. Chem.* **1986**, *302*, 181−191.

Table 1. ^{1}H, ^{13}C, and C−H Coupling Constants for Ti−Methyl Ligands

compound	^{1}H chemical shift of Ti−Me (δ in ppm)	^{13}C chemical shift of Ti−Me (δ in ppm)	$^1J_{C-H}$ (Hz)	reference
3	0.50	48.71	118.8	this work
4	0.691, 0.664	48.09, 47.78	120.9	this work
5	0.49, 0.46	49.53, 49.20		this work
Cp*TiMe$_2$(O-2,6-^{i}Pr$_2$C$_6$H$_3$)	0.81	54.2		43
Cp*TiMe$_3$	0.99	61.2	119	55
6	0.48		118.5	56

Table 2. Selected Bond Lengths (Å) and Bond Angles (deg) for 2

Bond Lengths	
Ti−Cp*(cent)	2.045(1)
Ti(1)−O(1)	1.7596(18)
N(1)−O(1)	1.417(3)
Ti(1)−Cl(1)	2.2980(5)
N(1)−C(1)	1.501(2)
Bond Angles	
Cl(1)−Ti(1)−Cl(1′)	103.83(3)
Cp*(cent)−Ti(1)−O(1)	122.46(3)
Cp*(cent)−Ti(1)−Cl(1)	113.04(2)
C(1)−N(1)−C(1′)	119.6(2)
Ti(1)−O(1)−N(1)	165.29(16)
O(1)−N(1)−C(1)	108.06
O(1)−Ti(1)−Cl(1)	101.09(4)

red complex **2**. In the latter case, use of excess reducing agent is essential to achieve high yields; use of stoichiometric amounts of reducing agent decreased the yield and led to recovery of substantial amounts of Cp*TiCl$_3$. Manganese powder is an ideal reagent for the single-electron reduction of Cp*TiCl$_3$ in THF in this synthesis, since excess manganese will not over-reduce the Cp*Ti(III) fragment and the MnCl$_2$ byproduct is insoluble in THF, thus facilitating simple removal by filtration.[49,50]

X-ray Crystallographic Analysis of Cp*TiCl$_2$(TEMPO) (2). Crystals of **2** suitable for single-crystal X-ray analysis were grown by slow cooling of a saturated toluene solution to −20 °C. Selected metrical parameters for this structure are given in Table 2, and the resulting ORTEP diagram is shown in Figure 1. (See Supporting Information for details of the data acquisition conditions and structure refinements.) X-ray analysis of **2** confirms the η^1-binding mode of the TEMPO ligand with a N−O bond length of 1.417 Å, consistent with an anionic TEMPO ligand as previously observed in the case of complex **1**.[46] The relatively short Ti−O bond length of 1.759 Å is similar to that previously observed in **1**. The overall complex exhibits C_s symmetry in the solid state, consistent with the observed solution ^{1}H NMR spectrum, with the C(6) methyl group located between the C(4) and C(4′) methyl groups of the TEMPO ligand. These steric interactions between the methyl groups of the Cp* and those of TEMPO force the Cp*(centroid)−Ti−O bond angle to widen from 117.6° in **1** to 122.5° in **2** and the Ti−O−N bond angle to increase from 155.7° to 165.3°. A similar widening of the Cp(centroid)−Ti−O bond angle in a series of Ti-aryloxide complexes has been previously noted when the Cp ligand carries substantial steric bulk.[44,51]

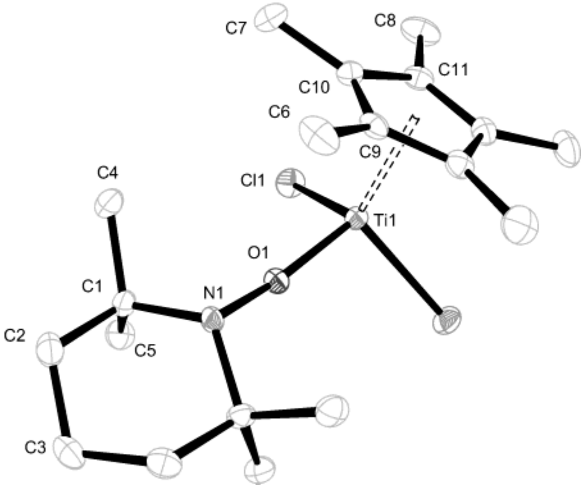

Figure 1. ORTEP diagram of (η^5-Cp*)TiCl$_2$(η^1-TEMPO) (**2**) with thermal ellipsoids at the 50% probability level.

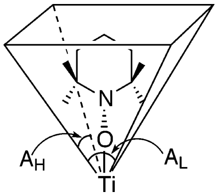

Figure 2. Illustration of the ligand wedge occupied by the TEMPO ligand which defines the ligand wedge angles A_L and A_H.

Table 3. Ligand Wedge Angles A_L and A_H Associated with Complexes 1 and 2 and Selected 2,6-Disubstituted Aryloxy Titanium Complexes Cp′TiCl$_2$(*O*-2,6-R$_2$Ar)

		CpTiCl$_2$(O-2,6-R$_2$Ar)			Cp*TiCl$_2$(O-2,6-R$_2$Ar)	
	1	R = Ph	R = ^{i}Pr	2	R = Ph	R = ^{i}Pr
A_L (deg)	131	157	123	134	148	121
A_H (deg)	88.3	59	94	88.5	53	92

Ligand cone angles are commonly used in organometallic chemistry to quantify the volume of space occupied by a ligand bound to a transition metal.[52] To more accurately describe ligands such as aryloxides that do not occupy a conical volume in space, Wolczanski proposed a modifed set of two parameters, angles A_L and A_H, that define the minimal pyramidal wedge that encompasses the van der Waals contacts of the ligand[53,54] (see Figure 2). From the crystal structure of **2** and the assumption that the van der Waals radius of each of the hydrogen atoms is 1.08 Å,[51] we find that the TEMPO ligand occupies a wedge having A_L = 134.0° and A_H = 85.5°. For consistency, we performed the same analysis with the previously reported crystal structure of **1** and found that A_L = 131.0° and A_H = 88.3°, which provides good agreement with the values obtained from **2**. Table 3 lists these values along with those determined for various titanium aryloxide complexes for comparison.[51]

---

(49) Williams, E. F.; Murray, M. C.; Baird, M. C. *Macromolecules* **2000**, *33*, 261−268.

(50) Mahanthappa, M. K.; Waymouth, R. M. *J. Am. Chem. Soc.* **2001**, *123*, 12093−12094.

(51) Sturla, S. J.; Buchwald, S. L. *Organometallics* **2002**, *21*, 739−748.

(52) Tolman, C. A. *Chem. Rev.* **1977**, *77*, 313−348.

(53) Wolczanski, P. T. *Polyhedron* **1995**, *14*, 3335−3362.

(54) Jafarpour, L.; Nolan, S. P. *J. Organomet. Chem.* **2001**, *617*, 17−27.

Comparison of these parameters shows that the η^1-TEMPO ligand exerts a steric influence comparable to that of 2,6-diisopropylphenoxide in the CpTi ligation environment. (For reference, the Tolman cone angle of the Cp ligand in **1** was determined to be 105.5° assuming that the van der Waals radius of a hydrogen atom is 1.08 Å.)

The alkylation chemistry of complex **2** was studied in some detail. Attempts to benzylate **2** with 2 equiv of PhCH$_2$MgCl in Et$_2$O at room temperature yielded a yellow-orange complex identified as Cp*TiCl(CH$_2$Ph)(TEMPO). ^{1}H NMR reveals a pair of doublets corresponding to the diastereotopic benzylic methylene protons having peak integrals consistent with the presence of only one benzyl ligand. Efforts to introduce a second benzyl group were unsuccessful in the presence of excess PhCH$_2$MgCl. ^{1}H NMR monitoring of the methylation of **2** with excess AlMe$_3$ in C$_6$D$_6$ at room temperature reveals the formation of a variety of species, including Cp*TiMe$_3$ (δ 1.74, 0.99 ppm)[55] and CH$_4$ (δ 0.16 ppm), indicating that the TEMPO ligand is susceptible to transmetalation by AlMe$_3$. Methylation of **2** proceeded sluggishly in reasonable yields using excess MeMgBr in Et$_2$O to provide the highly pentane soluble complex Cp*TiMe$_2$(TEMPO) (**3**), while use of MeLi in Et$_2$O resulted in traces of **3**. These results are consistent with a crowded steric environment created by the ligation of TEMPO to titanium, which may hinder facile alkylation.

NMR analyses of complexes **2** and **3** exhibit broadened ^{1}H NMR signals corresponding to the methyl groups of the TEMPO ligand, as well as broadened ^{13}C NMR resonances assigned to those primary carbons. These signals sharpen upon warming the sample to 70 °C. Since complementary broadening is not observed in the ^{1}H NMR signals of the Cp* ligand, we attribute these spectral features to a hindered ring inversion of the TEMPO ligand bound to the sterically bulky Cp*TiX$_2$ fragment. These observations are in contrast to the sharp ^{1}H and ^{13}C NMR resonances associated with **1**. The ^{1}H NMR resonance corresponding to the Ti–Me of **3** occurs at δ 0.50 ppm, significantly upfield from that of Cp*TiMe$_3$ (0.99 ppm); similarly, the ^{13}C NMR resonance for the Ti–Me in **3** occurs at δ 48.7 ppm as compared to the downfield shift observed for Cp*TiMe$_3$ (δ 61.2 ppm).[55] The $^1J_{\mathrm{C-H}}$ coupling constant of **3** is 118.8 Hz, compared to 118.0 Hz for MeSi$_2$(η^5-Me$_4$Cp)(η^1-N-*t*Bu)TiMe$_2$ (**6**)[56] and 119 Hz for Cp*TiMe$_3$ (Table 1).

The thermal stabilities of **1**–**3** in C$_6$D$_6$ were examined by ^{1}H NMR spectroscopy. Complexes **1** and **2** exhibit no evidence of decomposition upon heating to 70 °C for 4 h, even in the presence of CCl$_4$ at 70 °C in C$_6$D$_6$. The dimethyl complex **3** is also quite thermally stable, as evidenced by the lack of decomposition of this compound after heating at 70 °C in C$_6$D$_6$. The thermal stability of these complexes contrasts that recently reported for Cp$_2$TiCl(TEMPO), which undergoes homolysis of the Ti–O bond and a chlorine atom transfer reaction with CCl$_4$ at 60 °C in C$_6$D$_6$ to generate Cp$_2$TiCl$_2$ and TEMPO free radical.[57]

Nitroxide coordination complexes of titanium can also be prepared by salt metathesis reactions between titanium chlorides and anionic nitroxide equivalents, thus obviating the need to manipulate the oxidation state of titanium. Nitroxide anions are easily generated in situ under anaerobic conditions by the reaction of organolithium and organomagnesium reagents with nitrones.[58,59] Alkylation of *tert*-butyl-α-phenylnitrone with methyllithium in Et$_2$O generates a nitroxide anion which reacts with Cp′TiCl$_3$ to give Cp′TiCl$_2$[ON(^{t}Bu)(CHMePh)] (Cp′ = Cp or Cp*). While both synthetic routes give moderate yields on a preparative scale, the second method facilitates modular access to a wide variety of nitroxide ligand structures by judicious choice of the organolithium reagent or the nitrone; various nitrones may be synthesized from the condensation of alkylhydroxylamines with ketones and aldehydes.[58] Braslau and Hawker recently demonstrated the utility of this reaction sequence for the generation of libraries of alkoxyamine initiators for controlled/living free radical polymerization.[59] Therefore, the nitrone method provides a means of systematically varying the nitroxide and Cp ligand structure.

Alkylation of the *tert*-butyl-substituted nitroxide complexes with 2 equiv of methyllithium, followed by extraction and recrystallization from pentane, provides CpTiMe$_2$[ON(^{t}Bu)(CHMePh)] (**4**) in 55% yield; alkylation of the Cp* analogue yielded a pentane-soluble oil identified as Cp*TiMe2[ON(^{t}Bu)(CHMePh)] (**5**), which could not be obtained in analytically pure form due to its high solubility in pentane (Scheme 1B). Neutral complex **4** does not exhibit any instability toward β-H elimination or cyclometalation reactions in the temperature range 20–70 °C. NMR studies of **4** and **5** also reveal the magnetic inequivalence of the Ti–Me ligands which occur upfield relative to the methyl resonances of Cp*TiMe$_3$ in both ^{1}H and ^{13}C NMR spectra (Table 1).

The NMR spectra of the alkylated complexes **3**–**5** exhibit features that imply that the titanium center is electron rich. In particular, the chemical shifts of the Ti–Me groups fall in the range δ 0.70–0.50 ppm in C$_6$D$_6$, which is comparable to that observed for the constrained geometry complex **6** (δ 0.48 ppm) and upfield of that observed for Cp*TiMe$_3$ (δ 0.99 ppm).[55] The $^1J_{\mathrm{C-H}}$ coupling constants for the Ti–Me signals for **3** and **4** also provide an indirect measure of the electron density at the metal. Grubbs et al. previously proposed that the C–H coupling constant of the methyl group in a Ti–Me species can serve as a sensitive indicator of the electron density at titanium, where lower C–H coupling constants are indicative of a more electron-rich metal center.[60,61] By this criteria, the lower $^1J_{\mathrm{C-H}}$ for **3** and **6** indicates that these metal centers are more electron rich than the parent Cp*TiMe$_3$ and decrease in the order Cp*TiMe$_3$ < **3** < **6** (Table 1).

---

(55) Mena, M.; Royo, P.; Serrano, R.; Pellinghelli, M. A.; Tiripicchio, A. *Organometallics* **1989**, *8*, 476–482.

(56) Klosin, J.; Kruper, W. J.; Nickias, P. N.; Roof, G. R.; De Waele, P.; Abboud, K. A. *Organometallics* **2001**, *20*, 2663–2665.

(57) Huang, K. W.; Waymouth, R. M. *J. Am. Chem. Soc.* **2002**, *124*, 8200–8201.

(58) Lombardo, M.; Trombini, C. *Synthesis-Stuttgart* **2000**, 759–774.

(59) Benoit, D.; Chaplinski, V.; Braslau, R.; Hawker, C. J. *J. Am. Chem. Soc.* **1999**, *121*, 3904–3920.

(60) Finch, W. C.; Anslyn, E. V.; Grubbs, R. H. *J. Am. Chem. Soc.* **1988**, *110*, 2406–2413.

(61) Zachmanoglou, C. E.; Docrat, A.; Bridgewater, B. M.; Parkin, G.; Brandow, C. G.; Bercaw, J. E.; Jardine, C. N.; Lyall, M.; Green, J. C.; Keister, J. B. *J. Am. Chem. Soc.* **2002**, *124*, 9525–9546.

Table 4. Ethylene/Hexene Copolymerization Results with Monocyclopentadienyltitanium Complexes 3, 4, and 6 Activated with ^{ipr}AFPB[a]

complex	run	[Ti] (μM)	X_e/X_h[b]	yield (g)	prod ($\times 10^2$)[c]	$[E]_{copolymer}$ (mol %)[d]	% hexene conversion	M_w (kDa)[e]	M_n (kDa)[e]	M_w/M_n
3	1	52.8	0.0825	0.107	1.51	31.5	0.288	24.3	7.85	3.10
	2	52.8	0.119	0.159	2.24	45.1	0.351	133.8	47.4	2.82
	3	52.8	0.185	0.175	2.46	52.4	0.336	184.1	53.3	3.45
	4	52.8	0.299	0.249	3.44	63.3	0.368	188.2	63.3	2.97
4	5	50.0	0.187	0.315	4.73	45.9	0.686	37.9	16.1	2.35
	6	50.0	0.292	0.243	3.65	51.7	0.472	51.0	19.8	2.58
6	7	8.16	0.085	0.153	14.1	26.9	0.45	16.0	3.47	4.62
	8	12.3	0.125	0.097	78.9[f]	27.2	0.284	32.9	15.0	2.19
	9	11.1	0.185	0.272	55.1[g]	30.9	0.757	46.5	23.8	1.95
	10	12.5	0.305	0.334	20.0	38.8	0.822	78.2	36.0	2.17

[a] Polymerizations were carried out in 39 mL of 1-hexene + 1 mL of toluene containing 60 mg of triisobutylaluminum at 20 ± 1 °C for 20 min (see Experimental Section for copolymerization conditions). [b] Monomer feed ratio, where X_e = mole fraction ethylene, X_h = mole fraction 1-hexene. [c] Catalyst productivity in (kg polymer/mol Ti·h). [d] Determined by ^{13}C NMR. [e] Determined by gel permeation chromatography. [f] Polymerization time = 15 min. [g] Polymerization time = 6.67 min.

Synthesis of ^{ipr}AFPB. Since the initial discoveries by Ewen and Marks that organoboron compounds such as $B(C_6F_5)_3$ can serve as well-defined cocatalysts for the activation of group 4 coordination complexes for olefin polymerization, numerous other borate and aluminate activators have been synthesized.[62] Turner disclosed the use of $[PhNMe_2H][B(C_6F_5)_4]$, anilinium tetrakis(pentafluorophenyl)borate (AFPB), as an efficient activator in group IV metal mediated olefin polymerizations.[63,64] This acidic cocatalyst activates the transition metal precatalyst by protonolysis of one of the ligands to yield a cationic transition metal complex carrying a tetrakis(pentafluorophenyl)borate counteranion. AFPB, however, exhibits low solubility in hydrocarbon solvents and often requires long dissolution times in order to effect complete solubilization.

An anilinium borate activator derived from commercially available 2,6-diisopropyl-*N*,*N*-dimethylaniline was prepared as a more soluble analogue of $[PhNMe_2H][B(C_6F_5)_4]$. Treatment of 2,6-diisopropyl-*N*,*N*-dimethylaniline with anhydrous HCl in Et_2O yields the corresponding ammonium salt. Salt metathesis of this ammonium chloride with $(Et_2O)_{2.5}LiB(C_6F_5)_4$ in CH_2Cl_2 followed by filtration to remove the LiCl byproduct and pentane precipitation yields the product $[(2,6\text{-}^iPrC_6H_3\text{-}NMe_2H][B(C_6F_5)_4]$ (^{ipr}AFPB). The ^{1}H NMR spectrum of this compound in $CDCl_3$ reveals that the protonation of the sterically hindered aniline results in desymmetrization of the arene, giving rise to separate resonances for each of the isopropyl methyl and methine groups as well as the three aromatic protons. This new ^{ipr}AFPB activator exhibits higher solubility (~5 mg/mL) than the parent AFPB (~1 mg/mL) in toluene at 22 °C after a 12 h dissolution period with rapid stirring.

Ethylene/1-Hexene Copolymerizations of $CpTiX_2$(nitroxide) Complexes. The ethylene/1-hexene copolymerization behavior of methylated complexes **3** and **4** was investigated in the presence of two activators: ^{ipr}AFPB (in the presence of triisobutylaluminum (TIBA) as a scavenging agent) and Albemarle unmodified MAO. Copolymers having ethylene contents ranging from 32 to 65 mol % were obtained using a variety of ethylene/1-hexene feed ratios. The constrained geometry catalyst $MeSi_2(\eta^5\text{-}Me_4Cp)(\eta^1\text{-}N\text{-}^tBu)TiMe_2$ (**6**) was studied under the same conditions for comparison. The copolymerization results are shown in Table 4. Complexes **3** and **4** are active catalysts for the copolymerization of ethylene and 1-hexene to E/H copolymers having high 1-hexene contents. Ethylene/1-hexene copolymerizations using $Cp^*Ti(CH_2Ph)_3$ (**7**) under the same conditions yielded only traces of polymer which were insufficent for analysis. Thus the activities of these Cp′Ti(nitroxide) complexes are higher than those of the trialkyl complex **7**, indicating that the nitroxide ligand is essential for the enchanced productivities of **3** and **4** relative to **7**. These catalytic activites are, however, an order of magnitude lower than those of catalyst **6**.

The molecular weights of polymers produced by **4** are lower than those produced by **3**, which is likely a consequence of the less electron-rich Cp ligand in **4**, which results in a higher rate of chain transfer. This last observation is consonant with previous molecular weight trends observed by Nomura et al. in the case of MAO-activated Cp(aryloxy)Ti catalysts.[25] Copolymers derived from **3** and **4** under these conditions exhibit molecular weight distributions that are slightly broader than those expected for single-site catalysts (M_w/M_n = 2.35−3.10) and may be indicative of secondary reactions (such as transmetalation of the TEMPO ligand) leading to more than one active site. Nevertheless, the higher activity of **3** and **4** relative to **7** and the similarity of the GPC traces of **3**, **4**, and **6** under these activation conditions (see Supporting Information) provide good evidence that for the majority of the active species the nitroxide ligand remains bound to the transition metal under these activation conditions. This is in stark contrast to the behavior observed with MAO activators, where very broad and multimodal molecular weight distributions were observed (vida infra).

Comonomer feed compositions were determined using the empirical equation reported by Spitz et al.[65] for the solubility of ethylene in 1-hexene. To accurately estimate the kinetic copolymerization parameters r_e and r_h and the product r_er_h for all of these complexes, the copolymerizations were carried to low 1-hexene conversions (less than 1%) to avoid drift in the monomer feed ratio. Copolymer compositions and triad distributions were calculated according to the method of Cheng[66]

---

(62) Chen, E. Y. X.; Marks, T. J. *Chem. Rev.* **2000**, *100*, 1391−1434.

(63) Turner, H. W. Eur. Pat. Appl. 277004, 1988.

(64) Hlatky, G. G.; Upton, D. J.; Turner, H. W. PCT Int. Appl. 9109882, 1991.

(65) Spitz, R.; Florin, B.; Guyot, A. *Eur. Polym. J.* **1979**, *15*, 441−444.

(66) Cheng, H. N. *Polym. Bull.* **1991**, *26*, 325−332.

Table 5. Optimized Reactivity Ratios for Ethylene/1-Hexene Copolymerizations with Complexes 3, 4, and 6 Activated with ^{ipr}AFPB/TIBA at 20 °C

complex	N_{exp}[a]	X_e/X_h[b]	%E in copolymer[c]	r_e[d]	r_h[d]	$r_e r_h$[d]
3	4	0.0825−0.299	32.6−63.3	5.7 ± 0.9	0.13 ± 0.01	0.77 ± 0.14
4	2	0.187−0.292	45.9−51.7	3.1 ± 0.3	0.16 ± 0.02	0.50 ± 0.09
6	3	0.125−0.305	26.9−38.8	2.2 ± 0.2[e]	0.40 ± 0.10[e]	0.89 ± 0.24[e]

[a] Number of experiments used to calculate the average reactivity ratios. [b] Range of feed ratios over which the reactivity ratios are calculated. [c] Range of %E incorporations in the copolymers as determined by ^{13}C NMR analysis. [d] Optimized reactivity ratios and standard deviations were calculated according to the methods given in ref 76. [e] Calculated using runs 8−10 (Table 4).

using ^{13}C NMR assignments previously reported by Hsieh and Randall.[67,68] Reactivity ratios were calculated from the experimental data for each polymer produced using the experimentally determined triad distributions and the following equations:

$$r_e = \frac{k_{ee}}{k_{eh}} = \frac{2[EEE] + [EEH]}{(2[EHE] + [HHE])\frac{X_e}{X_h}}$$

$$r_h = \frac{k_{hh}}{k_{he}} = \frac{(2[HHH] + [HHE])\frac{X_e}{X_h}}{(2[EHE] + [HHE])}$$

where X_i denotes the mole fraction of monomer i in the copolymerization feed, and k_{ij} denotes the rate of insertion of monomer j into a polymer chain whose last inserted monomer unit is monomer i.[69]

From the reactivity ratios and triad distributions determined for each copolymer produced, optimized copolymerization probabilities P_{ij} (the probablility that monomer j inserts into a polymer chain ending in monomer i) were calculated over all feed ratios to achieve an optimized fit between the experimental triad distributions and those calculated from a first-order Markov model. Using these copolymerization probabilities, we calculated the optimized reactivity ratios over all feeds for each titanium complex from the following equations:[69]

$$r_e = \left(\frac{1}{P_{eh}} - 1\right)\frac{X_h}{X_h}$$

$$r_h = \left(\frac{1}{P_{he}} - 1\right)\frac{X_e}{X_h}$$

Detailed listings of the experimentally determined triad distributions and copolymerization reactivity ratios determined by ^{13}C NMR analysis for each polymer shown in Table 4 are given in the Supporting Information.

The optimized reactivity ratios and their products for complexes **3**, **4**, and **6** under ^{ipr}AFPB activation in the presence of TIBA are shown in Table 5. The experimentally derived values of r_e and r_h shown in Table 5 for **6** are in reasonable agreement with the values determined by Soga et al. in ethylene/1-octene copolymerization (r_e = 2.7 and r_o = 0.45).[70] The product of the reactivity ratios for each of the complexes ranges from 0.50 to 0.77, indicative of a slight tendency toward alternation.[71] Additionally, comparison of **3** and **4** demonstrates that reduction of steric crowding at the metal center by decreasing the steric bulk of both the Cp and the nitroxide ligands leads to higher 1-hexene incorporation with comparable catalytic activity.

The results in Tables 4 and 5 demonstrate that **3** and **4** in the presence of ^{ipr}AFPB/TIBA incorporate comonomer exceedingly well and at a level slightly lower than that of the constrained geometry catalyst **6**. From the crystallographic analysis of **2**, we find that the geometry of this complex is quite different from that of the constrained geometry complex $MeSi_2(\eta^5\text{-}Me_4Cp)(\eta^1\text{-}N\text{-}{}^tBu)TiCl_2$, **6**.[72] The Cp(centroid)−Ti−N bond angle of 107.6° in **6** is much smaller than the Cp(centroid)−Ti−O bond angle of 122.46° in **2**, implying a sterically unsaturated titanium center in **6**. Conversely, titanium is sterically well-protected in **2**, which may account for its sluggish reactivity in alkylation to form the dimethyl complex **3**. Differences in catalyst productivity between **3** and **6** in ethylene/1-hexene copolymerizations may derive from the steric bulk at the nitroxide-ligated titanium center in **3** and the complementary steric unsaturation of **6**. We find noteworthy the fact that the difference in productivity between **3** and **6** is not as large as that between **3** and **7**. This indicates that while the steric environment at the metal center does influence catalyst productivity, these effects are not nearly as profound as the effect of having a second monoanionic non-Cp ligand in the catalyst coordination sphere.

Previous studies of ethylene/α-olefin copolymerization using mono-Cp titanium complexes, especially those related to the constrained geometry catalysts[23,36−38] and $CpTiCl_2$(aryloxide) complexes,[25,42,43] have suggested that steric factors are important for controlling the comonomer selectivity. The hypothesis that sterically unencumbered ligand frameworks allow better accessibility to the titanium center for the bulky α-olefin comonomer, giving rise to high comonomer incorporations and high catalyst activities, is reasonable. Nevertheless, our results, and recent studies by Erker[33] and Stephan,[41] suggest that the ability of half-metallocene catalysts to incorporate α-olefin comonomers is not dictated solely by steric effects at the catalyst active site. The accumulating evidence from the literature suggests that monocyclopentadienyl titanium complexes possessing a suitable monanionic ligand can provide active

---

(67) Hsieh, E. T., Randall, J. C. *Macromolecules* **1982**, *15*, 1402−1406.

(68) Randall, J. C. *J. Macromol. Sci.- Rev. Macromol. Chem. Phys.* **1989**, *C29*, 201−317.

(69) Fink, G.; Richter, W. J. In *Polymer Handbook*, 4th ed.; Brandup, J., Immergut E. H., Grulke, E. A., Eds.; John Wiley & Sons: New York, 1999; Vol. II, pp 329−337.

(70) Soga, K.; Uozumi, T.; Nakamura, S.; Toneri, T.; Teranishi, T.; Sano, T.; Arai, T.; Shiono, T. *Macromol. Chem. Phys.* **1996**, *197*, 4237−4251.

(71) Odian, G. *Principles of Polymerization*; John Wiley & Sons: New York, 1991.

(72) Carpenetti, D. W.; Kloppenburg, L.; Kupec, J. T.; Petersen, J. L. *Organometallics* **1996**, *15*, 1572−1581.

Table 6. Ethylene/Hexene Copolymerization Results with Monocyclopentadienyltitanium Complexes 1, 2, and 4 Activated with Unmodified MAO[a]

complex	run	yield (g)	prod (× 10^2)[b]	$[E]_{copolymer}$ (mol %)[c]	% hexene conversion	M_w (kDa)[d]	M_n (kDa)[d]	M_w/M_n
1	11	0.071	1.05	82.3	0.051	213.0	9.38	22.7[e]
2	12	0.127	1.91	60.9	0.200	139.6	7.55	18.5[e]
4	13	0.161	2.20	55.0	0.29	53.2	13.4	3.96
Cp^*TiCl_3	14	0.083	1.25	77.2	0.076	62.2	2.71	22.9[e]

[a] Polymerizations were carried out in 39 mL of 1-hexene + 1 mL toluene at 20 ± 1 °C for 20 min with 0.970 MPa ethylene, $[Al]/[Ti] = 1000$ with unmodified MAO, $[Ti] = 50\ \mu M$, and $X_e/X_h = 0.188$ (see Experimental Section for copolymerization conditions). [b] Catalyst productivity in (kg polymer/mol Ti·h). [c] Determined by ^{13}C NMR. [d] Determined by gel permeation chromatography. [e] Bimodal GPC trace.

catalysts that can readily incorporate α-olefin comonomers.[25,27−31,40−42,73] These results suggest that for half-metallocenes, the strong σ-donating and possibly π-donating character of ligands such as nitroxides (this work), amides,[24,39] phosphinimides,[27,28,40,41] ketimides,[30,31] iminoimidazolidides,[29] and aryloxides[25,42−45] (compared to alkyl or halide coligands) may be equally important as steric effects in favoring high comonomer incorporations.

MAO Activation. We also examined the use of unmodified MAO as a cocatalyst in ethylene/1-hexene copolymerizations with complexes **1**, **2**, **4**, and Cp^*TiCl_3 at a single comonomer feed in order to determine the stability and behavior of these complexes as compared to those obtained with ^{ipr}AFPB/TIBA activation (see Table 6). The polymer produced by Cp^*TiCl_3/MAO under these conditions contains a higher amount of ethylene compared to that produced by **2**/MAO and exhibits a bimodal molecular weight distribution ($M_w/M_n = 22.9$). The copolymer produced by **2**/MAO has a substantially higher ethylene content than that produced by **3**/^{ipr}AFPB/TIBA at a similar E/H feed ratio and also possesses a bimodal molecular weight distribution ($M_w/M_n = 18.5$). The bimodal molecular weight distributions obtained for **1** and **2** in the presence of MAO suggest that activation of these complexes by MAO leads to multiple catalytic species that have different selectivities for ethylene and hexene. It is likely that under these activation conditions, transmetalation of the nitroxide by MAO can take place, leading to catalytic species similar to that obtained from Cp^*TiCl_3/MAO. This is consistent with the higher ethylene incorporations observed and with our stoichiometric experiments with **1** where $AlMe_3$ is able to remove the TEMPO ligand from titanium. Activation of **4** with MAO yields a polymer with a narrower molecular weight distribution than that observed for **1** and **2** ($M_w/M_n = 3.96$), indicating that the stability of these nitroxide ligands to transmetalation by MAO depends on the nature of the nitroxide ligand. Nevertheless, the higher ethylene incorporations observed in copolymers derived from **4**/MAO relative to **4**/^{ipr}AFPB/TIBA (run 5 vs run 13) and the slightly higher molecular weight distribution for **4**/MAO ($M_w/M_n = 3.96$) relative to **4**/^{ipr}AFPB/TIBA ($M_w/M_n = 2.35−2.58$) suggest that some transmetalation may be occurring for this complex as well in the presence of MAO. These observations illustrate a potential liability of the monocyclopentadienyl complexes containing "unconstrained" monoanionic ligands in the presence of MAO.[25,41,73]

Conclusions. We have demonstrated two versatile synthetic approaches for producing monocyclopentadienyl titanium complexes bearing a monoanionic ligand derived from a stable nitroxyl radical, and we have shown that these complexes serve as effective catalysts for the copolymerization of ethylene and 1-hexene to give copolymers having high comonomer contents. Comparison of the copolymerization behavior of $Cp^*TiMe_2(TEMPO)$ with $Cp^*Ti(CH_2Ph)_3$ reveals that the presence of the nitroxide ligand dramatically increases the activity and comonomer selectivity of these catalysts. The nitroxide ligands are of comparable steric size to sterically hindered aryloxide ligands and are readily generated by alkylation of nitrones. The ability of these monocyclopentadienyl complexes to incorporate large amounts of comonomer, comparable to that of the constrained geometry catalyst $MeSi_2(\eta^5\text{-}Me_4Cp)(\eta^1\text{-}N\text{-}^tBu)TiMe_2$, implies that the ability of half-metallocene catalysts to incorporate α-olefin comonomers is not dictated solely by steric considerations at the catalyst active site and that the electronic features of monoanionic coligands may be equally important in influencing comonomer selectivity.

Experimental Section

Materials. Standard Schlenk techniques and an MBraun Labmaster 100 drybox were used in handling all oxygen- and moisture-sensitive compounds. Pentane, toluene, and polymerization grade ethylene (99.5%) were dried by passage through columns containing alumina and degassed by passage through Q-5 copper catalyst (Engelhard), and tetrahydrofuran, diethyl ether, 1-hexene, benzene-d_6, and toluene-d_8 were vacuum transferred from Na/K alloy prior to use. TEMPO (Aldrich) was doubly sublimed at 1×10^{-5} Torr prior to use to remove oily residues. 2,6,-Diisopropyl-*N*,*N*-dimethylaniline, *tert*-butyl-α-phenylnitrone, 3.0 M CH_3MgBr in diethyl ether, 1.0 M $PhCH_2MgCl$ in Et_2O, Li_3N, manganese powder, and triisobutylaluminum were purchased from Aldrich and used without further purification. MeLi (1.6 M) in diethyl ether (low chloride content) was purchased from Acros Organics. $CpTiCl_3$ was purchased from Strem. Cp^*TiCl_3,[74] $Cp^*Ti(CH_2Ph)_3$,[55] and $MeSi_2(\eta^5\text{-}Me_4Cp)(\eta^1\text{-}N\text{-}^tBu)TiMe_2$[7575−76] were synthesized according to known procedures. $(Et_2O)_{2.5}LiB(C_6F_5)_4$ (80% pure, contaminated with LiCl) and 10% methylaluminoxane (MAO) solution in toluene were supplied by Albemarle Corporation. MAO was dried under vacuum (10^{-5} Torr at 45 °C) to remove solvent and residual trimethylaluminum prior to use.

^1H NMR spectra were recorded on Varian Unity Inova 300, XL-400, Gemini 400, and Unity Inova 500 spectrometers and were referenced relative to the residual protiated solvent peaks in the samples. ^{13}C NMR spectra were obtained at 125 MHz

---

[73] Nomura, K.; Fujii, K. *Macromolecules* **2003**, *36*, 2633−2641.

[74] Llinas, G. H.; Mena, M.; Palacios, F.; Royo, P.; Serrano, R. *J. Organomet. Chem.* **1988**, *340*, 37−40.

[75] McKnight, A. L.; Masood, M. A.; Waymouth, R. M.; Straus, D. A. *Organometallics* **1997**, *16*, 2879−2885.

[76] Reybuck, S. E.; Meyer, A.; Waymouth, R. M. *Macromolecules* **2002**, *35*, 637−643.

using a Varian Unity Inova 500 spectrometer or at 100 MHz using a Gemini 400 spectrometer. Elemental analyses were carried out at Desert Analytics Laboratory (AZ).

CpTiCl$_2$(TEMPO) (1). CpTiCl$_3$ (0.523 g, 1.54 mmol) in 40 mL of THF was added at room temperature to a slurry of Li$_3$N (0.0277 mg, 0.51 mmol) in 10 mL of THF over 30 s to generate a yellow-green solution, which gradually became dark green. After 2 h at room temperature, this solution was added quickly to a solution of TEMPO (0.374 mg, 1.54 mmol) in 15 mL of THF at −40 °C to give a red-brown solution. The cold bath was removed and the reaction allowed to stir at room temperature for 2 h. Removal of the reaction solvent in vacuo yielded a red solid, which was extracted with 50 mL of toluene. Upon filtration of the toluene solution and concentration to ∼15 mL, microcrystalline material began to precipitate. Cooling to −45 °C yielded a large polycrystalline mass. Yield: 388 mg (48%). ^{1}H NMR (400 MHz, C_6D_6, 19 °C): δ (ppm) 6.16 (s, 5H, Cp−H), 1.16 (s, 12H, −CH_3), 1.00−1.25 (m, 6H, −CH_2−CH_2−CH_2). ^{13}C{^{1}H} NMR (100 MHz, C_6D_6, 19 °C): δ (ppm) 119.8, 63.2, 39.4, 26.7, 16.6. Anal. Calcd for $C_{14}H_{23}NOTiCl_2$: C 49.44, H 6.82, N 4.12. Found: C 49.63, H 6.90, N 4.10.

Cp*TiCl$_2$(TEMPO) (2): Method 1. Cp*TiCl$_3$ (1.196 g, 4.13 mmol) in 80 mL of THF was quickly added to a slurry of Mn powder (0.547 g, 9.94 mmol) in 10 mL of THF. After 12 h, the dark green reaction with copious precipitate was filtered through Celite to yield a dark green solution, which was added to a solution of TEMPO (646 mg, 4.13 mmol) in 15 mL of THF to give an orange-brown solution. The cold bath was removed and the reaction allowed to stir at room temperature. After 12 h, the reaction solvent was removed in vacuo, and the resulting brown solid was extracted with 100 mL of toluene. Filtration and concentration of the toluene solution to 25 mL caused a red crystalline material to precipitate. The toluene solution was warmed to redissolve this material and then cooled to −45 °C for crystallization. Yield: 1.051 g (62%).

Cp*TiCl$_2$(TEMPO) (2): Method 2. Cp*TiCl$_3$ (0.724 g, 2.50 mmol) in 40 mL of THF was quickly added to a slurry of Zn powder (0.368 g, 5.63 mmol) in 10 mL of THF. After 1 h, a solution of TEMPO (0.400 g, 2.56 mmol) in 12 mL of THF was added to the green solution at room temperature to yield a red-brown solution. The reaction solvent was removed under reduced pressure after 7 h, and the resulting solid was extracted with 50 mL of toluene. Filtration of this solution and removal of the solvent in vacuo yielded a dark brown solid. Recyrstallization of this solid from toluene by slow cooling to −20 °C yielded dark red blocks suitable for single-crystal X-ray analysis; Table 7 provides some details regarding crystal data as well as data collection and analysis. Yield: 0.507 g (49%). ^{1}H NMR (400 MHz, C_6D_6, 19 °C): δ (ppm) 2.00 (s, 15H, C(CH$_3$)$_5$)), 1.24−1.34 (m, 16H, −CH_3 and −(CH$_3$)C−CH_2−CH$_2$), 1.14 (m, 2H, CH$_2$−CH_2−CH$_2$). ^{13}C{^{1}H} NMR (125 MHz, C_6D_6, 60 °C): δ (ppm) 130.3, 64.3, 40.7, 27.3, 17.4, 12.8. Anal. Calcd for $C_{19}H_{33}NOTiCl_2$: C 55.63, H 8.11, N 3.41. Found: C 56.04, H 8.49, N 3.21.

Cp*TiCl(CH$_2$Ph)(TEMPO). Cp*TiCl$_2$(TEMPO) (0.414 g, 1.01 mmol) was slurried in 40 mL of Et$_2$O at 0 °C. By syringe, PhCH$_2$MgBr (2.0 mL, 2.00 mmol) was added dropwise in the dark over 3 min, causing the brown crystals to dissolve, yielding a dark red solution. The reaction was warmed to room temperature and stirred for 13.5 h. The reaction solvent was removed in a vacuum to yield a brown solid, which was extracted with 60 mL of hexanes and filtered. Concentration of the solution under vacuum to 10 mL and cooling to −72 °C yielded orange-red microcrystals. Yield: 0.190 g (40%). ^{1}H NMR (400 MHz, C_6D_6, 19 °C): δ (ppm) 7.37 (d, 2H, $^3J_{H-H} = 7.75$ Hz, −CH$_2$-*o*-Ph), 7.20 (app t, 2H, −CH$_2$-*m*-Ph), 6.91 (t, 1H, $^3J_{H-H} = 7.0$ Hz, −CH$_2$-*p*-Ph), 2.78 (d, 1H, $^2J_{H-H} = 7.0$ Hz, −CH_2Ph), 2.15 (d, 1H, $^2J_{H-H} = 7.0$ Hz, −CH_2Ph), 1.85 (s, 15H, C$_5$(CH_3)$_5$) 1.10−1.30 (m, 12H, −CH_2− and −CH_3), 0.80−1.00 (br s, 6H, −CH_3).

Table 7. Crystallographic Data for the X-ray Structural Analysis of 2

A. Crystal Data	
emp formula	$C_{19}H_{33}NOCl_2Ti$
dimens, mm	0.49 × 0.19 × 0.05
cryst syst	orthorhombic
space group	*Pnma*
a (Å)	15.3312(4)
b (Å)	14.4636(4)
c (Å)	9.4817(2)
V (Å^3)	2102.51(8)
Z	4
fw	410.28
density (g/cm^3)	1.296
μ, cm^{-1}	6.67
F_{000}	872.00
B. Data Collection and Structural Analysis	
scan type	ω (0.3°/frame)
scan rate (deg/min)	1.8
2θ range (deg)	49.3
no. of reflns	9332
no. unique reflns	1829
agreement factor	0.046
no. of observations ($I > 3\sigma(I)$)	1829
abs corr	Lorentz−polarization
R$_1$:*w*R$_2$ (1543 reflns $I > 4\sigma(I)$)	0.031
R$_1$:*w*R$_2$ (all data)	0.076
σ_1, goodness of fit	1.03
no. of variables	125
data to param ratio	14.63
largest diff peak and hole, e/Å^3	0.24, −0.40

Cp*TiMe$_2$(TEMPO) (3). Cp*TiCl$_2$(TEMPO) (0.505 g, 1.23 mmol) was slurried in 30 mL of Et$_2$O at 0 °C. By syringe, MeMgBr (1.8 mL, 5.4 mmol) was added dropwise over 5 min. The reaction was warmed to room temperature and stirred for 1 h. The reaction solvent was removed under reduced pressure to yield a yellow solid, which was extracted with 50 mL of pentane and filtered. Removal of the solvent under vacuum yielded a pale yellow solid, which was recrystallized from pentane at −50 °C. Yield: 0.198 g (46%). ^{1}H NMR (400 MHz, C_6D_6, 19 °C): δ (ppm) 1.87 (s, 15H, C(CH_3)$_5$), 1.43 (m, 6H, −CH_2−), 1.33 (s, 12H, −CH_3), 0.50 (s, 6H, Ti−CH_3). ^{13}C NMR (100 MHz, C_6D_6, 19 °C): δ (ppm) 120.8, 61.69, 48.71 ($^1J_{C-H} = 118.7$ Hz), 40.26, 26.84, 17.43, 11.37. Anal. Calcd for $C_{21}H_{39}NOTi$: C 68.28, H 10.64, N 3.79. Found: C 67.90, H 10.65, N 3.58.

CpTiMe$_2$(ON(^{t}Bu)(CHPhMe) (4). MeLi (2.0 mL, 3.2 mmol) was added dropwise over 4 min to a solution of *tert*-butyl-α-phenylnitrone (0.568 g, 3.2 mmol) in Et$_2$O at −78 °C. The reaction was warmed to room temperature and stirred for 5 h. This solution was then added to a room-temperature solution of CpTiCl$_3$ (0.701 g, 3.2 mmol) in Et$_2$O at room temperature to yield a red-brown solution. After 12 h, this reaction was cooled to −60 °C, and MeLi (4.0 mL, 6.4 mmol) was added dropwise by syringe to yield a yellow solution. The reaction was warmed to room temperature over 90 min and the solvent removed in vacuo. The resulting yellowish paste was extracted with 65 mL of pentane and filtered to yield a brilliant yellow solution. Removal of the solvent under vacuum and recrystallization from pentane at −45 °C yielded a yellow microcrystalline product. Yield: 0.592 g (55%). ^{1}H NMR (500 MHz, C_6D_6, 19 °C): δ (ppm) 7.43 (app d, 2H, $^3J_{H-H} = 7.5$ Hz, *o*-C$_6$H$_5$), 7.16 (m, 2H, *m*-C$_6$H$_5$), 7.07 (app t, 1H, $^3J_{H-H} = 7.5$ Hz, *p*-C$_6$H$_5$), 5.74 (s, 5H, Cp-H), 4.19 (q, 1H, $^3J_{H-H} = 6.5$ Hz, −NCHPhCH$_3$), 1.56 (3H, d, $^3J_{H-H} = 6.5$ Hz, NCHPhCH_3), 1.13 (9H, s, (CH$_3$)$_3$CN−), 0.691 (s, 3H, Ti−CH_3), 0.664 (s, 3H, Ti−CH_3). ^{1}H NMR (500 MHz, CDCl$_3$, 19 °C): δ (ppm) 7.53 (d, 2H, $^3J_{H-H} = 7.5$ Hz, *o*-C$_6$H$_5$), 7.36 (app t, 2H, $^3J_{H-H} = 7.5$ Hz, *m*-C$_6$H$_5$), 7.30 (app t, 1H, $^3J_{H-H} = 7.5$ Hz, *p*-C$_6$H$_5$), 5.94 (s, 5H, Cp-*H*), 4.49 (q, 1H, $^3J_{\mathrm{H-H}} = 6.5$ Hz, −NC*H*PhCH$_3$), 1.70 (3H, d, $^3J_{\mathrm{H-H}} = 6.5$ Hz, NCHPhC*H*$_3$), 1.27 (9H, s, (CH$_3$)$_3$CN−), 0.417 (s, 3H, Ti−C*H*$_3$), 0.388 (s, 3H, Ti−C*H*$_3$). ^{13}C NMR (100 MHz, C$_6$D$_6$, 19 °C): δ (ppm) 145.01, 128.73, 127.05, 113.47, 61.82, 60.825, 48.09 ($^1J_{\mathrm{C-H}} = 121.03$ Hz), 47.78 ($^1J_{\mathrm{C-H}} = 121.03$ Hz), 27.54, 17.43. ^{13}C NMR (100 MHz, CDCl$_3$, 19 °C): δ (ppm) 144.65, 128.43, 127.83, 126.76, 113.08, 61.96, 60.65, 47.67, 47.19, 27.54, 17.33. Anal. Calcd for C$_{19}$H$_{29}$NOTi: C 68.05, H 8.72, N 4.18. Found: C 67.68, H 8.94, N 3.98.

Cp*TiMe$_2$(ON(^{t}Bu)(CHPhMe)) (5). Synthesis is analogous to that of **4** except that Cp*TiCl3 (0.921 g, 3.18 mmol) and ^{t}Bu-α-phenylnitrone (0.564 g, 3.18 mmol) were used. Yield: not taken. ^{1}H NMR (500 MHz, C$_6$D$_6$, 20 °C): δ (ppm) 7.55 (d, 2H, $^3J_{\mathrm{H-H}} = 8.0$ Hz, *o*-C$_6$H$_5$), 7.2 (app t, 2H, $^3J_{\mathrm{H-H}} = 9.5$ Hz, *m*-C$_6$H$_5$), 7.09 (app t, 1H, $^3J_{\mathrm{H-H}} = 9.5$ Hz, *p*-C$_6$H$_5$), 4.38 (q, 1H, $^3J_{\mathrm{H-H}} = 8.5$ Hz, −NC*H*PhCH$_3$), 1.78 (s, 15H, (C(C*H*$_3$))$_5$), 1.67 (3H, d, $^3J_{\mathrm{H-H}} = 8.5$ Hz, NCHPhC*H*$_3$), 1.15 (9H, s, (C*H*$_3$)$_3$CN−), 0.49 (s, 3H, Ti−C*H*$_3$), 0.46 (s, 3H, Ti−C*H*$_3$). ^{13}C{^{1}H} NMR (125 MHz, C$_6$D$_6$, 20 °C): δ (ppm) 145.56, 128.16, 127.82, 127.49, 120.73, 62.84, 62.14, 49.53, 49.20, 27.64, 19.51, 11.38. This sample could not be obtained in analytically pure form due to its high degree of pentane solubility.

2,6-Diisopropyl-*N*,*N*-dimethylanilinium Tetrakis(pentafluorophenyl)borate ($^{\mathrm{ipr}}$APFB). Excess anhydrous gaseous HCl (generated by the dehydration of concentrated HCl(aq) and with concentrated H$_2$SO$_4$) was bubbled through a solution of 2,6-diisopropyl-*N*,*N*-dimethylaniline (2.0 g, 9.74 mmol) in 25 mL of Et$_2$O at room temperature to generate a white precipitate. The resulting anilinium hydrochloride was filtered on a medium frit in air, and the solid was washed with Et$_2$O (3 × 10 mL) to remove any excess aniline and dried under vacuum for 12 h at room temperature. Yield: 1.3 g (55% based on the aniline).

A 100 mL Schlenk tube was charged with 2,6-diisopropyl-*N*,*N*-dimethylanilinium chloride (0.588 g, 2.43 mmol) and (Et$_2$O)$_{2.5}$LiB(C$_6$F$_5$)$_4$ (80% purity) (2.503 g, 2.59 mmol) as solids, and 60 mL of dry CH$_2$Cl$_2$ was added at room temperature under nitrogen. After stirring for 72 h at room temperature, the reaction was Schlenk filtered through Celite and the filter cake was washed with 120 mL of CH$_2$Cl$_2$. The solvent was removed under vacuum from the combined filtrates to yield a bubbly, white solid. This solid was treated with 10 mL of CH$_2$Cl$_2$ and 100 mL of pentane to precipitate the solid white product, which was collected by filtration and washed with pentane (3 × 50 mL). ^{1}H NMR (500 MHz, CDCl$_3$, 19 °C): δ (ppm) 7.65 (br s, 1H, N−*H*), 7.54 (dd, 1H, $^3J_{\mathrm{H-H}} = 7.75$ Hz, $^3J_{\mathrm{H-H}} = 8.0$ Hz, *p*-C$_6$H$_3$), 7.44 (dd, 1H, $^3J_{\mathrm{H-H}} = 8.0$ Hz, $^4J_{\mathrm{H-H}} = 1.5$ Hz, *m*-C$_6$H$_3$) 7.32 (dd, 1H, $^3J_{\mathrm{H-H}} = 7.75$ Hz, $^4J_{\mathrm{H-H}} = 1.5$ Hz, *m*-C$_6$H$_3$), 3.46 (s, 3H, N−C*H*$_3$), 3.45 (s, 3H, N−C*H*$_3$), 3.13 (qq, 1H, $^3J_{\mathrm{H-H}} = 7.0$ Hz, $^3J_{\mathrm{H-H}} = 6.5$ Hz, −C*H*(CH$_3$)$_2$), 2.85 (qq, 1H, $^3J_{\mathrm{H-H}} = 7.0$ Hz, $^3J_{\mathrm{H-H}} = 6.5$ Hz, −C*H*(CH$_3$)$_2$), 1.39 (d, 3H, $^3J_{\mathrm{H-H}} = 6.5$ Hz, −CH(C*H*$_3$)(CH$_3$)), 1.34 (d, 3H, $^3J_{\mathrm{H-H}} = 7.0$ Hz, −CH(CH$_3$)(C*H*$_3$)). ^{13}C{^{1}H} NMR (125 MHz, CDCl$_3$, 19 °C): δ (ppm) 149.07, 147.16, 141.16, 139.16, 138.67, 137.23, 135.34, 132.20, 129.16, 125.86, 47.66, 29.66, 29.22, 24.01, 23.62. Anal. Calcd for C$_{38}$H$_{24}$NBF$_{20}$: C 51.55, H 2.73, N 1.58. Found: C 51.74, H 2.98, N 1.70.

Ethylene−Hexene Copolymerization Procedure: $^{\mathrm{ipr}}$AFPB Activation. All polymerizations were carried out in a 300 mL stainless steel autoclave equipped with a mechanical stirrer. Polymerizations employing $^{\mathrm{ipr}}$AFPB activation were carried out as follows: 60 mg of triisobutylaluminum (TIBA) dissolved in 35 mL of 1-hexene was loaded into a 150 mL double-ended injection tube equipped with quick-connect fittings. The autoclave was evacuated on a vacuum line and flushed four times with 100 psi of gaseous ethylene. The reactor was vented to 10 psig, and the TIBA/hexene solution was injected into the reactor under the desired ethylene pressure. Then this solution was allowed to equilibrate with rapid stirring for at least 30 min with a continuous ethylene feed. In a drybox, a stock solution of titanium organometallic compound (∼0.5−1 mg/mL 1-hexene) and a stock solution of $^{\mathrm{ipr}}$AFPB (1−3 mg/mL toluene) were prepared. The desired amount of stock solution containing the titanium complex was diluted with 1-hexene to a total volume of 2 mL and loaded into a 25 mL double-ended injection tube, while the desired amount of $^{\mathrm{ipr}}$AFPB stock solution was diluted with 1-hexene to a total volume of 3 mL and loaded into a 50 mL double-ended injection tube. The polymerization was initiated as follows: autoclave stirring was halted, the ethylene feed was disconnected, the reactor was vented by 10 psi, and the solution of organotitanium complex was injected under ethylene pressure. Once the pressure reached a maximum (15 s), the reactor was vented by 10 psi for a second time, and the $^{\mathrm{ipr}}$AFPB solution was introduced under ethylene pressure; stirring of the reactor was recommenced upon the second injection. The polymerizations were maintained at a constant temperature (±1 °C) using an ethylene glycol/water cooling loop. After a set reaction time, polymerizations were quenched by injection of 10 mL of methanol under argon pressure (250 psi) while slowly venting the reactor. The contents of the reactor were subsequently poured into a solution of methanolic HCl and stirred for 12 h. Tacky polymers were allowed to settle overnight to ensure complete product isolation. The acidic methanol was decanted and the resulting polymer was rinsed twice with 50 mL of methanol, followed by drying in a vacuum oven at 60 °C for at least 8 h.

MAO Activation. All polymerizations were carried out in a 300 mL stainless steel autoclave equipped with a mechanical stirrer. MAO (100 mg) was suspended in 35 mL of 1-hexene and was loaded into a 150 mL double-ended injection tube equipped with quick-connect fittings. The autoclave was evacuated on a vacuum line and flushed four times with 100 psi of ethylene. The reactor was vented to 10 psig, and the MAO/1-hexene suspension was injected into the reactor under the desired ethylene pressure. This solution was allowed to equilibrate under continuous ethylene feed with rapid stirring for at least 30 min. In a drybox, a stock solution of titanium organometallic compound (∼0.5−1 mg/mL 1-hexene) was prepared. The desired amount of stock solution containing the titanium complex was diluted with 1-hexene to a total volume of 2 mL and loaded into a 25 mL double-ended injection tube. The polymerization was initiated by disconnecting the ethylene feed, venting the reactor by 10 psi, and injecting the solution of organotitanium complex under ethylene pressure. The polymerizations were maintained at a constant temperature (±1 °C) using an ethylene glycol/water cooling loop. After a set reaction time, the polymerizations were quenched by injection of 10 mL of methanol under argon pressure (250 psi) while slowly venting the reactor. The reactor contents were poured into a solution of methanolic HCl and stirred for 12 h. Tacky polymers were allowed to settle overnight to ensure complete product isolation. The acidic methanol was decanted, and the resulting polymer was rinsed twice with 50 mL of methanol, followed by drying in a vacuum oven at 60 °C for at least 8 h.

Polymer Characterization. ^{13}C{^{1}H} NMR spectra (75.4 MHz) were obtained on a Varian Unity Inova 300 spectrometer using a 10 mm broad-band probe operating at 100 °C. Samples were prepared as solutions of 80 mg of polymer in 2.5 mL of 90:10 (*v*/*v*) 1,2-dichlorobenzene/benzene-*d*$_6$ containing ∼2 mg of chromium(III) acetylacetonate as a spin lattice relaxation agent. An inverse-gated decoupled pulse sequence with a pulse repetition delay of 5 s was used to acquire a minimum of 3000 transients per sample. Weight and number average molecular weights (M_{w} and M_{n}) were obtained by gel permeation chromatography using a Waters 150C high-temperature GPC operating at 140 °C in 1,2,4-trichlorobenzene equipped with seven Polymer Labs Mixed-A columns at a flow rate of 1.0 mL/min. A molecular weight calibration curve was constructed with 18 atactic polystyrene standards using a differential refractive index detector.

Acknowledgment. We gratefully acknowledge financial support from the NSF (NSF-CHE 9910240). M.K.M. acknowledges graduate fellowship support from the Fannie and John Hertz Foundation. We also thank Joyce Hung for help with statistical analyses of the copolymers, and the Albemarle Corporation for the generous gift of MAO and organoboron cocatalysts.

Supporting Information Available: Text giving the experimental details associated with data collection and refinement and tables of crystal data, positional parameters, anisotropic thermal factors, bond distances, bond angles, and torsional angles for **2**, and triad distributions for the entries in Tables 3 and 4 used to calculate experimental and optimized reactivity ratios. This material is available free of charge via the Internet at http://pubs.acs.org.

OM034096S